

## Li mobility in $(\text{Li,Na})_y\text{La}_{0.66-y/3}\text{TiO}_3$ perovskites ( $0.09 < y \leq 0.5$ ). A model system for the percolation theory.

*J. Sanz<sup>1</sup>, A. Rivera<sup>1,2</sup>, C. León<sup>2</sup>, J. Santamaría<sup>2</sup>, A. Várez<sup>3</sup>, O. V'yunov<sup>4</sup>, A.G. Belous<sup>4</sup>,*

<sup>1</sup> Instituto Ciencia de Materiales de Madrid - CSIC, 28049 Cantoblanco, Spain.

<sup>2</sup> GFMC, Dpto. Física Aplicada III, Universidad Complutense, 28040 Madrid, Spain.

<sup>3</sup> Dpto. Ciencia de Materiales. Universidad Carlos III de Madrid. 28911 Leganés, Spain.

<sup>4</sup> Solid State Chem., Inst. Inorg. Chem., Ukrainian Academy Sciences, 252680, Ukraine.

### ABSTRACT

The dependence of ionic transport on structure and composition of perovskites  $\text{Li}_y\text{La}_{0.66-y/3}\text{TiO}_3$  ( $0.09 \leq y \leq 0.5$ ) and  $\text{Li}_{0.5-x}\text{Na}_x\text{La}_{0.5}\text{TiO}_3$  ( $0 \leq x \leq 0.5$ ) has been analyzed by means of Neutron Diffraction, NMR and Impedance Spectroscopy. In the first series, ion conductivity displays a non-Arrhenius behavior, decreasing activation energy at increasing temperatures. Li mobility is accompanied by a considerable increase of Li thermal factor deduced from ND data. In the second series, local lithium mobility decrease monotonously with the sodium content at room temperature; however, long-range dc conductivity decreases sharply at  $x = 0.2$  more than six orders of magnitude. This decrease on dc conductivity is discussed in terms of a three-dimensional percolation theory of vacant A-sites. In this model, the number of vacant sites is controlled by the amount of Na and La of the perovskite.

### INTRODUCTION

Interest in ionic conducting solids is increasing in the last years because of their potential application as solid electrolytes in batteries, fuel cells and other electrochemical devices[1].  $\text{Li}_y\text{La}_{0.66-y/3}\text{TiO}_3$  perovskites, with  $0.09 < y < 0.5$ , are among the best Li ion conductors, showing a dc conductivity of  $10^{-3}$  S/cm at room temperature[2,3]. Since the discovery of its outstanding electrical properties, several groups have investigated structural features of these perovskites; however, reasons that enhances Li mobility have not been completely identified.

X-ray diffraction patterns of LLTO perovskites have been interpreted assuming a doubled perovskite along the c-axis ( $\mathbf{a}_p, \mathbf{a}_p, 2\mathbf{a}_p$  unit cells); however the symmetry changes along the series, from orthorhombic (S.G. Pmmm) to tetragonal (S.G. P4/mmm), when the Li content increases[3-5]. In samples quenched from 1350 °C, unit cell becomes cubic with parameters  $\mathbf{a}_p, \mathbf{a}_p, \mathbf{a}_p$  (S.G. Pm3m) [4,6]. These changes of symmetry are related to the cation vacancies ordering. In Li-poor samples, cation vacancies are disposed in alternating planes along the c-axis; however, in Li-rich samples, vacancies become disordered. For samples quenched from high temperature the highest disordering is achieved[6].

The octahedral tilting was analyzed with neutron diffraction. The structural analysis of the Li-poor  $\text{Li}_{0.18}\text{La}_{0.61}\text{TiO}_3$  perovskite, confirmed that vacant A-sites are disposed in alternated planes along the c-axis. Moreover, an octahedral tilting along the  $\mathbf{b}$  axis

produced the observed  $2a_p \times 2a_p \times 2a_p$  superstructure[7-9]. Neutron diffraction pattern of the quenched Li-rich member  $\text{Li}_{0.5}\text{La}_{0.5}\text{TiO}_3$  was described with the rhombohedral unit cell  $\sqrt{2}a, \sqrt{2}a, 2\sqrt{3}a$  (S.G. R-3c). In this sample, octahedral tilting was produced along the three axes and vacancies were fully disordered[6]. Substitution of Li by Na does not affect unit cell dimensions of rhombohedral perovskites. In these samples, Na ions occupy A sites of the perovskite while Li ions are located at the center of the square planar windows connecting contiguous A sites[10].

In order to analyze structural factors that affect transport properties in lanthanum titanates perovskites, we have studied solid solutions  $\text{Li}_y\text{La}_{0.66-y/3}\text{TiO}_3$  ( $0.09 \leq y \leq 0.5$ ) and  $\text{Li}_{0.5-x}\text{Na}_x\text{La}_{0.5}\text{TiO}_3$  ( $0 \leq x \leq 0.5$ ) (LLTO and LNLTO series). This study has been carried out by neutron diffraction (ND), Nuclear Magnetic Resonance (NMR) and Impedance Spectroscopy (IS). In particular, short and long-range mobilities were analyzed with NMR and IS techniques.

## EXPERIMENTAL

Samples were obtained from stoichiometric amounts of dried  $\text{Li}_2\text{CO}_3$  (Merck),  $\text{Na}_2\text{CO}_3$  (Merck),  $\text{La}_2\text{O}_3$  (Aldrich 99.99%) and  $\text{TiO}_2$  (Aldrich 99 %) by solid state reaction, following the procedure used in previous works[4,10]. The mixture was grounded together in an agate mortar and heated at 800 °C for 4 hours in order to eliminate  $\text{CO}_2$ . The reground products were cold-pressed at 150 MPa and heated at 1150 °C for 12 hours. Finally, LNLTO and LLTO samples were pressed and heated at 1200 °C and 1350 °C (6 h) respectively.

$^7\text{Li}$  and  $^{23}\text{Na}$  NMR spectra were obtained at room temperature in a MSL-400 Bruker spectrometer working at 155.45 MHz and 104.8 MHz respectively. Spectra were taken after irradiation of the sample with a  $\pi/2$  pulse (3  $\mu\text{s}$ ). Spin-spin relaxation times ( $T_2$ ) were deduced from the linewidth of the spectra. Spin-lattice relaxation times ( $T_1$ ) were measured between 170 K and 500 K by using the classical ( $\pi$ - $\tau$ - $\pi/2$ ) sequence in a SXP 4/100 Bruker spectrometer, working at 10.6 MHz.

Sintered cylindrical pellets 5 mm in diameter and 1 mm thick, with evaporated silver electrodes, were used for electrical measurements. Impedance Spectroscopy measurements were conducted between 125 K and 330 K, using precision LCR meters HP4284A and HP4285A in the frequency range 20 Hz - 30 MHz. These measurements were carried out under  $\text{N}_2$  flow to ensure an inert atmosphere.

## RESULTS AND DISCUSSION

### *Li mobility in $\text{Li}_y\text{La}_{0.66-y/3}\text{TiO}_3$ series*

Figure 1 shows the plot of dc conductivity versus reciprocal temperature for orthorhombic and tetragonal perovskites,  $\text{Li}_y\text{La}_{0.66-y/3}\text{TiO}_3$  ( $y = 0.18$  and  $0.5$ ). Both samples present a similar behavior, displaying activation energies that progressively decrease from 0.4 to 0.26 eV, when temperature increases. In analyzed series, dc conductivity increases with the Li content, reaching a *plateau* for  $y > 0.25$ [4].

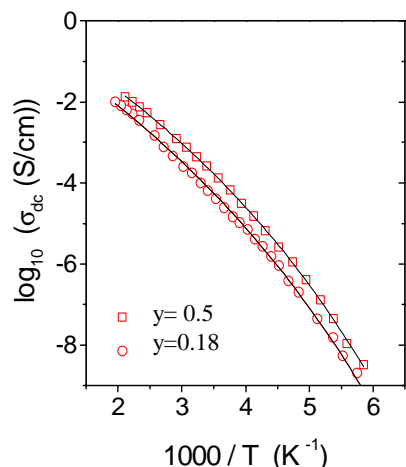


**Figure 1.-** Arrhenius plot of dc-conductivity of LLTO samples with  $y = 0.18$  and  $0.5$

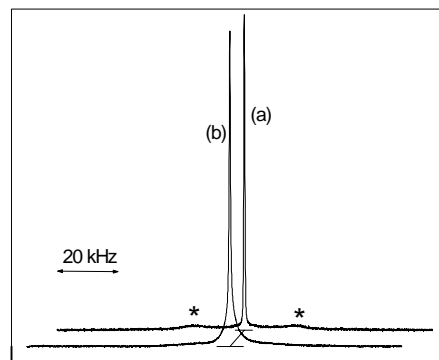


**Figure 2.-** R.T.  $^7\text{Li}$  NMR spectra of LLTO samples with (a)  $y = 0.18$  and (b)  $y = 0.5$ .

$^7\text{Li}$  ( $I=3/2$ ) NMR spectra of  $\text{Li}_{0.18}\text{La}_{0.61}\text{TiO}_3$  (a) and  $\text{Li}_{0.5}\text{La}_{0.5}\text{TiO}_3$  (b) are given in figure 2. The spectrum of the Li-poor sample,  $x = 0.18$ , is formed by the central and two satellite transitions. The analysis of Li NMR spectra showed the presence of two lithium species with different mobility that exchange their positions to give a mean quadrupolar constant,  $C_Q \sim 60$  kHz, at room temperature[7]. In Li-rich samples ( $y = 0.5$ ), only a single component with very low  $C_Q$  was detected, indicating that mobile species predominate in this perovskite[11]. ND experiments of this samples, showed that Li ions were four-fold coordinated to oxygens in a planar square configuration occupying the center of the square windows that connect contiguous A-sites of the perovskite[6].

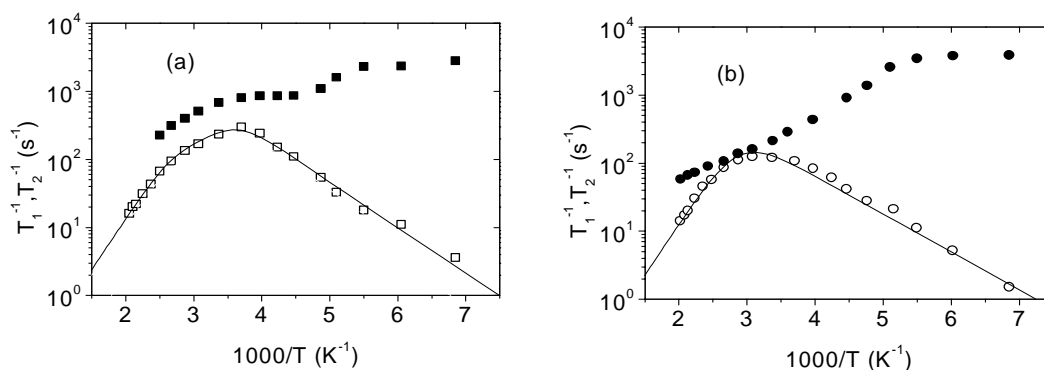


**Figure 3.-** Temperature dependence of  $T_1^{-1}$  (open symbols) and  $T_2^{-1}$  (solid symbols) for samples with  $y=0.18$  (a) and  $y=0.5$  (b).

In figure 3,  $^7\text{Li}$  spin-lattice ( $T_1^{-1}$ ) and spin-spin ( $T_2^{-1}$ ) relaxation rates of  $\text{Li}_{0.18}\text{La}_{0.61}\text{TiO}_3$  (a) and  $\text{Li}_{0.5}\text{La}_{0.5}\text{TiO}_3$  (b) perovskites are plotted versus reciprocal temperature. In both samples, Li mobility increases considerably above 180K, producing a considerable decrease of the linewidth ( $T_2^{-1}$ ) with temperature. In the case of orthorhombic samples, the decrease of  $T_2^{-1}$  values is not monotonous, observing a *plateau* between 200-300 K. This behavior has been ascribed to the existence for lithium of a two-dimensional motion in ordered samples[4,7,12]. At this point, it is interesting to compare square windows that connect contiguous A sites of the perovskites. ND data showed that these

windows display diagonal O-O distances  $\approx 3.65$ - $4.15$  Å in the rhombohedral but  $\approx 3.64$ - $3.88$  and  $3.89$ - $4.13$  Å in the orthorhombic sample[8,9]. Taken into account the higher amount of vacancies in the plane  $z/c=0.5$  than in  $z/c=0$ , it is reasonable to assume a two-dimensional motion for lithium in orthorhombic samples. At high temperatures, Li motion becomes three-dimensional. In the case of the rhombohedral samples, Li motion is three-dimensional.

In analyzed samples, a maximum of  $1/T_1$  is detected at temperatures near 300 K, evidencing high mobility of lithium ions in two perovskites. At this temperature, the residence time of Li ions at structural sites is near  $10^{-8}$  s. In two analyzed cases,  $T_1^{-1}$  curves display three regimes. Below 200 K, Li motion is basically localized inside unit cells of perovskite. Between 200 and 370 K, Li ions pass through square windows that connect contiguous A-sites, preserving the Li motion a localized character. Above 370 K, Li motion becomes extended and a long range ionic transport is achieved[11,12]. In  $\text{Li}_{0.5}\text{La}_{0.5}\text{TiO}_3$  sample, the last two regimes are poorly resolved.

Localization of lithium at unit cell faces of the perovskite, deduced from difference Fourier maps in  $\text{La}_{0.5}\text{Li}_{0.5}\text{TiO}_3$ , decreases considerably at increasing temperatures. Above 573 K, localization of Li becomes difficult with diffraction techniques (see Fig. 4). Taken into account that conductivity is similar in all analyzed  $\text{Li}_y\text{La}_{0.66-y/3}\text{TiO}_3$  perovskites, we can conclude that the octahedral tilting and distribution of vacancies do not limit seriously Li diffusion in LLTO perovskites.

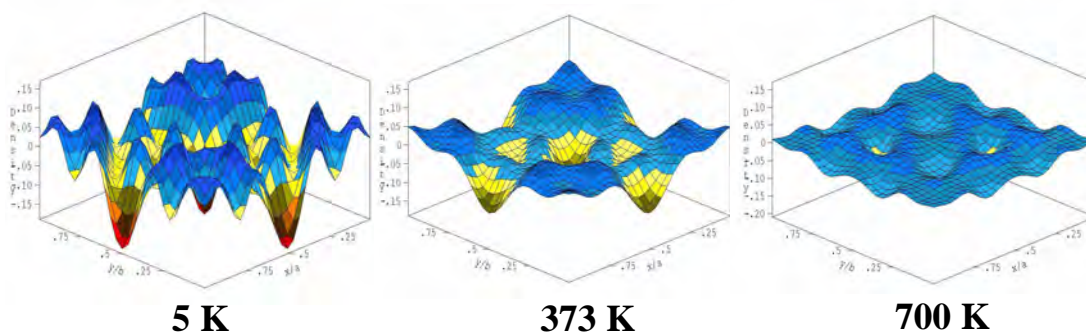


**Figure 4.** Difference Fourier maps at  $z=0$  in  $\text{La}_{0.5}\text{Li}_{0.5}\text{TiO}_3$ . Detected minima correspond to Li ions, not included in the refinement model. Localization of Li becomes difficult at increasing temperatures.

#### *Li mobility in $\text{Li}_{0.5-x}\text{Na}_x\text{La}_{0.5}\text{TiO}_3$*

$^7\text{Li}$  MAS-NMR spectra of  $\text{Li}_{0.5-x}\text{Na}_x\text{La}_{0.5}\text{TiO}_3$  perovskites showed that the central line is more intense than that would correspond to satellite transitions (modulated by equally spaced lateral bands), indicating the presence of mobile species whose concentration decreases in a monotonous way with the sodium content (Figure 5a).  $^7\text{Li}$  MAS NMR spectra of less mobile species were fitted with the same parameters than in LLTO series ( $C_Q = 60$  kHz,  $\eta = 0.5$ ), suggesting that  $\text{Li}^+$  ions occupy similar positions in both series. In Na-rich samples, most Li displays very low mobility. However, conductivity  $\sigma_{dc}$  values in LNLTO series showed an abrupt decrease at  $x = 0.31$  that cannot be explained

in terms of the number of charge carriers,  $n_c$  (Figure 5b). This fact evidences the critical effect of Na on the long-range ionic transport in LNLTO perovskites.

In a recent study of the  $\text{Li}_{0.5-x}\text{Na}_x\text{La}_{0.5}\text{TiO}_3$  ( $0 \leq x \leq 0.5$ ) series, it was shown that all samples display a rhombohedral R-3c symmetry, with unit cell parameters that do not change appreciably with the composition[10]. The octahedral tilting produces Ti-O-Ti angles near  $167^\circ$  and an oblique distortion of square windows that connect contiguous A sites of the perovskite, impeding Na ions to pass through windows. If Li ions were located at the A sites, the amount of vacant A-sites and conductivity should be very low in this series. However, dc conductivity of Li-rich samples ( $x < 0.2$ ) is very high at room temperature, suggesting that A-sites associated with Li are not occupied and Li pass through square windows.

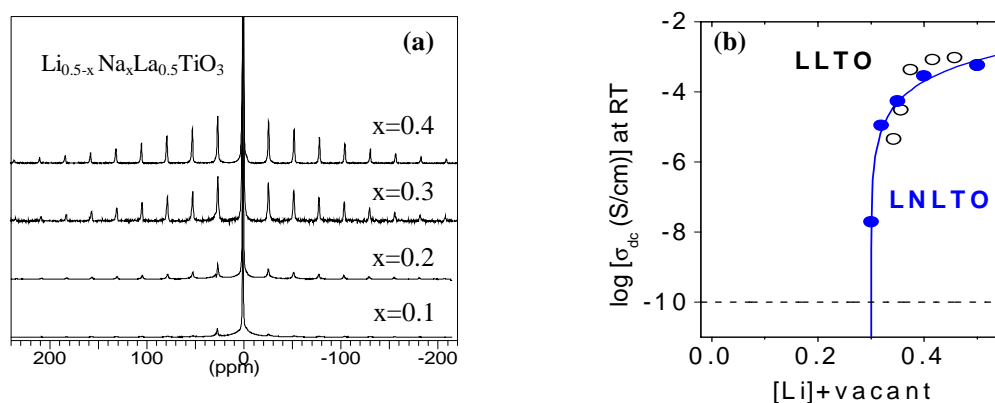


**Figure 5.- (a)**  $^7\text{Li}$  MAS-NMR spectra of  $\text{Li}_{0.5-x}\text{Na}_x\text{La}_{0.5}\text{TiO}_3$  perovskites with increasing amount of sodium **(b)**  $\sigma_{dc}$  vs. Li plus vacant sites in LLTO and LNLTO.

Taken into account that Na occupy preferentially A-sites, we have considered a percolation model in which A sites associated with Li ions are vacant and participate in ionic diffusion, but  $\text{La}^{3+}$  and  $\text{Na}^+$  ions occupy A sites blocking conduction pathways of the perovskite[10]. In this model, vacant distribution is random and dc conductivity is given by the expression  $\sigma_{dc} = K(n - n_p)^2$ , where  $n$  is the number of vacant A-sites and  $n_p$  is the percolation threshold for a three-dimensional cubic network ( $n_p \approx 0.31$ ). In agreement with these predictions, ion conductivity is very high when the sodium content is lower than 0.2, but very low above this value. At  $x = 0.2$ , the amount of vacancies is close to the percolation threshold, and conductivity decreases drastically (see Figure 5b)[10,13].

Based on structural and spectroscopic results, the amount of vacant A-sites could correspond to the sum of nominal vacancies plus Li content. The plot of dc-conductivity vs Li + vacancies is given in the Figure 4b. Conductivity values of LLTO and LNLTO series agree with those deduced from the percolation model, confirming that sites A associated with lithium ions are vacant and participate to Li conduction. According to this fact, the amount of vacancies in LLTO samples (0.3-0.5) is higher than the percolation threshold and conductivity of all these samples is important. In the case of LNLTO series, the amount of vacancies decrease below the percolation threshold and dc-conductivity decrease dramatically.

## CONCLUSIONS

Cation mobility has been studied in crystalline  $\text{Li}_y\text{La}_{0.66-y/3}\text{TiO}_3$  ( $0.09 \leq y \leq 0.5$ ) and  $\text{Li}_{0.5-x}\text{Na}_x\text{La}_{0.5}\text{TiO}_3$  ( $0 \leq x \leq 0.5$ ) perovskites by means of NMR and Impedance spectroscopies. In the first series, modifications produced in bottlenecks by tilting of octahedra do not affect seriously Li diffusion. In these perovskites, Li occupies unit cell faces of the perovskite, increasing the number of vacant A-sites that participate in Li motion. In orthorhombic perovskites, distribution of vacancies favors the two-dimensional motion of Li.

In  $\text{Li}_{0.5-x}\text{Na}_x\text{La}_{0.5}\text{TiO}_3$  perovskites, Na and La ions are located at A sites, reducing the amount of vacant A sites that participate in ion motion. According to this fact,  $\sigma_{dc}$  conductivity display a sharp decrease at  $x = 0.2$  that has been ascribed to a percolation of Li motion along the conduction paths. In LLTO samples, the amount of vacant A-sites,  $0.33 \leq n_v \leq 0.5$ , is always bigger than the percolation threshold and conductivity displays high values. In LNLTO samples, the number of vacant sites decreases below the percolation threshold and conductivity decreases drastically.

## ACKNOWLEDGMENTS

Financial support from CICYT through MAT98 1053-C03 and MAT2001 3713-C03 projects is acknowledged. Authors thank J.A. Alonso and M.T. Fernández-Díaz for helpful discussions and ILL for provision of neutron beam time.

## REFERENCES

1. K. M. Colbow, J. R. Dahn, R. R. Hearing, *J. Power Sources* **26**, 397 (1989).
2. A. G. Belous, G. N. Novitskaya, S. V. Polyanetskaya, Yu. I. Gornikov, *Izv. Akad. Nauk SSSR, Neorg. Mater.* **23**, 470 (1987).
3. Y. Inaguma, C. Lique, M. Itoh, T. Nakamura, T. Uchida, H. Ikuta, M. Wakihara, *Solid State Commun.* **86**, 689 (1993).
4. J. Ibarra, A. Várez, C. León, J. Santamaría, L.M. Torres-Martínez, J. Sanz, *Solid State Ionics* **134**, 219 (2000).
5. J. L. Fourquet, H. Duroy, M.P. Crosnier-Lopez, *J. Solid Stat. Chem.* **127**, 283 (1996).
6. J. A. Alonso, J. Sanz, J. Santamaría, C. León, A. Várez, M. T. Fernández-Díaz, *Angew. Chem. Int. Ed.* **39**, 619 (2000).
7. M. A. París, J. Sanz, C. León, J. Santamaría, J. Ibarra, A. Várez, *Chem. Mat.* **12**, 1694 (2000).
8. J. Sanz, J. A. Alonso, A. Várez, M. T. Fernández-Díaz, *J. Chem. Soc. Dalton Trans.* 1406 (2002).
9. Y. Inaguma, T. Katsumata, M. Itoh, Y. Morii, *J. Solid State Chem.* **166**, 67 (2002).
10. A. Rivera, C. León, J. Santamaría, A. Várez, O. V'yunov, A. G. Belous, J. A. Alonso, J. Sanz, *Chem. Mat.* (2002) (in press).
11. C. León, J. Santamaría, M. A. París, J. Sanz, J. Ibarra, L. M. Torres, *Phys. Rev. B* **56**, 5302, (1997).
12. A. Rivera, C. León, J. Santamaría, A. Várez, M. A. París, J. Sanz, *J. Non-Crystalline Solids* **307-310**, 992 (2002).
13. Y. Inaguma, M. Itoh, *Solid State Ionics* **86-88**, 257 (1996).